Does the earth have an adaptive infrared iris?

Richard S. Lindzen, MIT,
Ming-Dah Chou, GSFC, and Arthur Hou, GSFC

Preliminary draft
February 18, 2000

Abstract

Observations and analyses of water vapor and clouds in the tropics over the past decade suggest a different approach to radiative climate feedbacks: namely, that high clouds and high free-tropospheric relative humidity are largely tied to each other, and that the main feedback consists in changing the relative areas of cloudy/moist regions vis a vis clear/dry regions in response to the surface temperature of the cloudy/moist regions – as opposed to altering the humidity in either of the regions. This is an intrinsically 2-dimensional (horizontal and vertical) effect which does not readily enter simple 1-dimensional (vertical) radiative-convective schemes which emphasize average humidity, etc. Preliminary analyses of cloud data for the eastern part of the Western Pacific from the Japanese GMS-5(Geostationary Meteorological Satellite), are supportive of this suggestion – pointing to a 15% reduction in cloudy/moist area for a 1C increase of the sea surface temperature as measured by the cloud-weighted SST (sea surface temperature). The implication of this result is examined using a simple 2-dimensional radiative-convective model. The calculations show that such a change in the tropics would lead to a strong negative feedback in the global climate, with a feedback factor of about -1.7, which, if correct, would easily dominate the positive water vapor feedback found in current models. This new feedback mechanism, in effect, constitutes an adaptive infrared iris that opens and closes in order to control the OLR (outgoing longwave radiation) in response to changes in surface temperature in a manner similar to the way in which an eye's iris opens and closes in response to changing light levels. The climate sensitivity resulting from this thermostatic mechanism is consistent with the independent determination by Lindzen and Giannitisis (1998). Preliminary attempts to replicate observations with GCMs (General Circulation Models) suggest that models lack such a negative cloud/moist areal feedback.

1. Introduction.

Observations and analyses over the past decade allow us to plausibly limit the possibilities for water vapor and/or cloud climate feedbacks – at least in the tropics. Indeed, as we shall see, cloud and water vapor feedbacks are, to an important extent, inseparable.

Much of our current understanding of both the greenhouse effect and the role of atmospheric feedbacks comes from one-dimensional models of the sort used by Manabe and Wetherald (1967). Here, the atmosphere is characterized by a single vertical distribution of water vapor, and a specified mean cloud cover consisting in clouds at one or more levels. However, in recent years, satellites have provided detailed pictures of the horizontal distribution of water vapor at various levels. Figure 1 illustrates such a distribution obtained by Spencer and Braswell for May 5, 1995 for the layer 500-300mb from 183GHz microwave radiation observed from the SSM/T-2

military satellite (Spencer and Braswell, 1997, show similar results for a monthly mean; however, we wished to show a daily map as opposed to a monthly mean since radiation responds to the instantaneous distribution.). Although microwave retrievals are less sensitive to the presence of clouds, similar results were obtained from TOVS infrared soundings (Stephens et al, 1996). Results for all levels above 700mb are similar. Below 700mb we have the turbulent trade wind boundary layer in the tropics where humidity tends to be relatively high everywhere. What we see is that the tropics above the boundary layer consist in regions which are very dry and regions which are very moist. The transition between the two is sharp; this sharpness is not apparent in monthly means.

The dry regions are generally regions of large scale subsidence. The moist regions are more complicated. While they tend to be regions of large scale ascent, the ascent is concentrated in cumulus towers which have small areal coverage (Riehl and Malkus, 1958, Held and Soden, 2000). The bulk of the moist regions consists in descending air which is moistened by the evaporation of precipitation from high cirrus, and, at levels below about 500mb, by dissipating cumuli (Gamache and Houze, 1983, Betts, 1990, Sun and Lindzen, 1993). In general, in the tropics, high stratiform clouds are the source of high humidity, and the production of high cirrus depends on the microphysics of rain formation within the cumulus towers (Emanuel and Pierrehumbert,1996, Sun and Lindzen, 1993). Condensed water vapor which does not form rain, freezes and is available to form cirrus anvils. The situation is schematically illustrated in Figure 2.

Consistent with the role of high cirrus clouds in moisturizing the tropical troposphere, Udelhofen and Hartmann (1995) find a close correspondence between upper level cloudiness and high relative humidity. For monthly means, they find that high relative humidity is confined to within 500 km of the cloudy regions. However, for daily retrievals the correspondence is tighter. Radiation, of course, responds to the instantaneous values of radiatively active substances rather than to their means. High clouds can be measured with high spatial and temporal resolution from geostationary satellites. The measurement of relative humidity, on the other hand, is difficult in the presence of clouds and requires somewhat ambiguous 'cloud-clearing' algorithms. The above results, however, suggest that upper level cloudiness can be taken as a surrogate for high relative humidity, thus obviating the need to explicitly measure the area of high humidity. Note that in this view, the traditional cloud and water vapor feedbacks are inextricably tied to each other.

A number of recent studies (Sherwood, 1996, Soden, 1998, Salathé and Hartmann, 1997) have shown that in the dry regions of Figure 1, the water vapor budget is in largely advective balance with no evidence of any other sources at all. This strongly limits the possibilities for altering the humidity of dry regions, and observations suggest that these regions may be about as dry as they can get (Spencer and Braswell, 1997). In addition, the moist tropical regions in Figure 1 are nearly saturated, suggesting that there is little scope for changing humidity in these regions as well.

If there is little scope for significantly altering the humidity of the moist and dry regions, then the main remaining possibility for a significant feedback lies in changing the relative areas of

cloudy/moist and clear/dry air in response to changes in surface temperature. Given the sharp transition between moist and dry regions shown in Figure 1, we may plausibly expect that shrinking (growing) cloudy/moist areas are accompanied by growing (shrinking) clear/dry areas. In section 2, we discuss this possibility in more detail, and in section 3, we describe how we can use high resolution cloud observations to evaluate these feedbacks, and present some preliminary results for the period January 1998 - August 1999. The observationally based coincidence of cloudy and moist regions substantially facilitates the observational and subsequent theoretical analysis. A very strong inverse relation is found between cloudy/moist area and the mean SST of cloudy regions (which we refer to as the cloud-weighted SST). Section 4 uses a simple 2-dimensional radiative-convective model to estimate climate feedbacks from the observed relation between cloudy/moist area and cloud-weighted SST. Section 5 compares the observed behavior with the behavior of a number of current models. Section 6 discusses possible implications for climate as well as the limitations of the present analysis.

2. Reassessment of the possibilities for atmospheric feedbacks.

The above results tend to limit the possibility for atmospheric feedback in the tropics to changes in the relative areas of the clear/dry and cloudy/moist regions. Dynamics effectively homogenizes temperature in the horizontal, so that the clear/dry regions act to cool the whole tropics. Such a situation was graphically described by Pierrehumbert (1995) among others. Eddies act to couple the tropics to the rest of the globe. Note that the commonly used categorization of feedbacks into separate water vapor and cloud feedbacks stems largely from the one-dimensional models of the sort used by Manabe and Wetherald (1967). The area feedback we propose to examine is intrinsically two dimensional.

The area feedback hinges on the factors which determine cirrus detrainment from cumulus towers. In general, detrainment of ice depends on the water substance carried by cumulus updrafts which is *not* rained out within the tower. Feedbacks will depend on the specific impact of surface temperature. In general, coalescence proceeds more rapidly as the temperature of the cumulonimbus cloud increases (Sun and Lindzen, 1993, Rogers and Yau, 1989); thus, increasing temperature, itself, will act to reduce cirrus outflow. However, other microphysical processes play a role, and simple coalescence is likely to underestimate the effect of temperature when account is taken of stochastic effects as well as the drag exerted on cloud updrafts by falling rain. In view of these complexities, we, therefore, attempt to ascertain feedbacks directly from data. Our procedure will be, following the findings of Udelhofen and Hartmann (1995), to use upper cloud coverage as a surrogate for the area of the cloudy/moist regions, and to study how this area varies with the surface temperature weighted according to cloud coverage. We weight the temperature according to cloud coverage because cloud microphysics depends only on the temperature beneath the clouds and not the average temperature over the whole domain. The origin of such temperature changes depends among other things on the time interval considered. Thus, over short periods of a week or so, SST varies relatively little (over most regions), and cloud-weighted SST changes mostly due to clouds, whose lifetime is measured in hours, popping up in different locations characterized by different SST as illustrated schematically in Figure 3. Over longer periods, the situation is more complex. Not only are there changes in SST, but changing patterns in surface temperature (Lindzen and Nigam, 1987) and propagating internal

waves (Miller and Lindzen, 1992, Straus and Lindzen, 2000) lead to varying distributions of low level convergence and shifting patterns of convection. Theoretically, given the short time scales associated with cloud processes, it seems likely that the dependence of the area of cloudy/moist air on cloud-weighted SST should not depend greatly on the specific origin of the changes in cloud-weighted SST (i.e., whether the temperature changes were associated with varying positions of clouds or with actual changes in SST). However, within limited regions, the seasonal and interseasonal changes in regime can, in principle, alter the overall level of convection within the region. Thus, shorter periods (on the order of a month) might be more suitable for determining specifically cloud physics related behavior. As we will see, however, this can be checked by examining brightness temperatures corresponding to the tops of cumulonimbus towers.

For time scales of months to years (including ENSO), changes in SST are irregular, and there need be no particular relation between changes in cloud-weighted SST and domain-averaged surface temperature. Indeed, as we will note in Section 3, the former are much larger. However, for global change due to doubling CO_2, global mean temperature might be suitable since presumably almost all temperatures are proportional (at least in models). Even here, the physically relevant temperature change for the area of the cloudy/moist region will be the cloud-weighted surface temperature. It bears emphasizing that the physics (precipitation formation, etc.) determining the area of the cloudy/moist regions is fast, and hence such changes in area can be measured from short period fluctuations. However, it is the same fast physics which determines the response to long period fluctuations.

The need to average over the entire globe is rigorously necessary only for items like energy and water substance which satisfy budget relations (Lindzen, 1990), and where one needs to average out horizontal transport. This is *not* the case for high cloud area vs. cloud weighted surface temperature. *Here, regions can, in principle, contribute independently.*

3. Explicit observational results.

We wish next to examine the data to determine whether a significant feedback exists in the form of a response of the area of cloudy/moist air to changes in the cloud-weighted SST. Given the discussion in Section 1, the regions of upper level cloudiness and high humidity coincide to a large extent. Thus, one can simply measure high cloud coverage as a surrogate for cloudy/moist regions. This is the procedure we will follow here, though it might be just as effective to retrieve free tropospheric humidity while counting regions obscured by clouds to be humid. An advantage of measuring clouds is the existence of 11 and 12μ channels which can be used to detect clouds (Prabhakara et al, 1993) on geostationary satellites which obtain data with high temporal and spatial resolution over fixed regions. Unfortunately, archives of most such data are not readily available. However, we have been able to archive data from the Japanese GMS satellite since January 1998. When clouds are viewed with high time and space resolution, they appear very patchy with the patches moving about very substantially over short periods. Given the physics illustrated in Figure 2, we expect that these clouds will moisturize the air between close by patches. Thus the cloud area measured on an hourly basis will be taken as indicative of the area of cloudy/moist air but not numerically equal to this area. This should suffice for the

present since our aim is not so much to produce a definitive analysis as to obtain some idea of the existence and magnitude of the effect. As mentioned earlier, because of the sharp observed transition between cloudy/moist and clear/dry regions we expect that increasing (decreasing) cloudy/moist area to be accompanied by equally decreasing (increasing) clear/dry area. The situation with respect to surface temperature is somewhat more problematic. The primary available data set is the NCEP data compiled by Reynolds and Smith (1994) from ship track and satellite observations. Here the spatial resolution is 1 degree by 1 degree and the time resolution is 1 week. The Reynolds-Smith data suggests that the spatial variation is smooth and changes little from week to week which suggests, in turn, that it can safely be interpolated to match the higher resolution cloud data. Although this is the procedure we will follow for the present preliminary assessment, we are aware that there are regions where SST has a strong diurnal variation (at least in skin temperature) that is not accounted for here (Fairall et al, 1996). While this may prove to be a problem, the air temperature is more relevant for cloud microphysics, and this temperature has a smaller diurnal variation.

We have, so far, examined high cloud over the region 30S-30N, 130E-170W using cloud data from GMS-5 and NCEP (National Center for Environmental Prediction) SST for 20 months (1 January 98 - 31 August 99). The region is shown in Figure 4. The region encompasses a wide variety of situations – especially in the course of 20 months. Cloud data is available from 5x5km pixels with hourly time resolution. The SST data, as already noted, is much coarser with spatial resolution of 1 degree by 1 degree (latitude and longitude) and weekly time resolution. However, at least within the NCEP data set, SST varies slowly compared to the cloud time scales (of order 10 hours) and relatively smoothly with respect to distance. For a heavily ocean covered region, we may plausibly expect clouds to be responding to surface temperature; over land, the situation is likely to be more complicated since surface temperatures can respond rapidly to clouds. We, therefore, restrict ourselves to the simpler primarily oceanic regions in this paper. Of course, reference to Figure 4 shows that even the region we are looking at includes some land (as well as the maritime continent). This (plus unincluded daily variations in SST) are expected to add scatter to our results, and make the detection of any relation more uncertain. Nevertheless, the relations we find seem to be sufficiently robust to suggest that this is not too serious a problem.

Japan's GMS is located above the Equator and 140◄E longitude. To estimate high-level clouds covering both day and night, only the brightness temperatures measured at the split-window channels (11 and 12 μ) are used. A GMS pixel is determined to be either clear or totally covered by clouds by comparing the brightness temperatures at the 11-μ channel (T_{11}) to a subjectively selected threshold temperature, T_{th}. For thick high clouds, the difference between the brightness temperatures at the 12-μ channel (T_{12}) and T_{11} is small, which can be used to differentiate thick clouds from thin clouds (Prabhakara, et al., 1993). This threshold temperature difference, dT, depends upon the spectral ranges of the split window channels. For the GMS channels, dT is empirically chosen to be 1.5 K. Hourly high cloud amount in a 1◄x1◄latitude-longitude region is estimated using the 5-km resolution pixels.

The displacement of cloud systems depends on large-scale conditions. The time scale of clouds is much smaller than that of the sea surface temperature (SST). When the cloud systems appear in a warm oceanic region, they are expected to be modified by the SST nearly immediately. SST

will also respond to clouds, but at a much slower pace. Thus, the modification of clouds by local SST can be studied by correlating high cloud amount to the local SST.

For a large oceanic domain, the mean high-cloud amount and the mean SST beneath high clouds are computed from

$$A = \sum_n A_n$$

$$\bar{T} = \frac{\sum_n A_n T_n}{A}$$

where A is the cloud amount, T is the SST and the subscript n denotes $1 \ll 1$ <latitude-longitude regions.

The results for the 20 month period are shown in panels (a) and (b) of Figure 5. Panel (a) corresponds to Channel 11's brightness temperature being less than 260K, corresponding to upper level clouds, while panel (b) shows the subset of clouds in panel (a) for which the Channel 12 brightness temperature is within 1.5K of Channel 11 which, as we discussed earlier, corresponds to thicker clouds. Several points should be noted: 1) the coverage of thicker clouds is considerably less than the coverage of all clouds; and 2) panels (a) and (b) both show a reduction of cloud amount by about 45% for an increase of cloud-weighted SST of 3K which suggest that both measures are proportional to overall cloudiness. In order for our interpretation of Figure 5 as an indication of the dependence of detrainment on the temperature of the surface beneath the clouds to be correct, two further conditions must be met. The *first condition* is that there be no systematic change in the amount of cumulus convection; otherwise, the changes we see might simply reflect changes in cumulus activity (as might be caused by changes in low level convergence due to either seasonal changes in SST pattern or the penetration into the tropics of extratropical systems) rather than detrainment. Figure 6 shows the dependence of cloud coverage for Channel 11 brightness temperature less than 220K. Here we are looking at the cold tops of cumulonimbus towers. We no longer see a clear reduction with increasing cloud weighted temperature; indeed there is a small and probably insignificant increase. This confirms that what we see in Figure 5 is due to varying detrainment from cumulus convection rather than any change in the amount of cumulus convection itself. This is *essential* in isolating the effect we are seeking. That is to say, one can only attribute changes in the area of cloudy/moist area to changes in cloud-weighted SST in cases where the amount of convection, itself, is not changing significantly with cloud-weighted temperature. Indeed, the fact that cumulus convection appears to have been increasing slightly, suggests that the area effect in Figure 5 is likely to be somewhat *underestimated*, since increasing convection would generally lead to more rather than less upper level cloudiness. We should also note that for cumulus towers there is no difference in areal coverage when we restrict ourselves to thicker clouds, which is to say that all cumulus towers are thick. The small areal coverage for cumulus towers even within the cloudy regions (ca 2%) is consistent with the early findings of Riehl and Malkus (1958) – especially when one considers that at any given moment, most cumulus tops represent dying rather than active cumulus. The *second condition* is that the regions of cumulus activity and cirrus coverage largely coincide.

Otherwise the conceptual picture illustrated in Figure 2 would be inappropriate. For example, if purely stratiform clouds were to intrude into the tropics as part of an extratropical weather system, we would obtain both an decrease in cloud-weighted SST and an increase in stratiform cloud area. We examine this by checking whether the results in Figures 5 and 6 depend on whether we use SST weighted by clouds for which the brightness temperature is less than 260K or less than 220K. The results turn out to be essentially identical, confirming that both cumulus and cirrus exist in the same regions – at least over the scales characteristic of SST variation.

We also examined deviations from domain- and monthly-averaged values. This amounts to essentially compositing monthly variations by removing inter-monthly variations. The results are shown in panels (c) and (d) of Figures 5 and 6. The results are essentially the same as obtained for the 20-month series, though the scatter is much reduced. For the monthly composites, changes in cloud-weighted SST arise primarily from clouds appearing in regions of differing SST rather than changes in SST itself.

Finally, we should also note that cloud-weighted SST varies much more with time than either SST or mean SST. The fact that cloud microphysics depends on cloud-weighted SST gives us a much larger dynamic range to examine, which, in turn, is important for reliable determination of the effect of cloud-weighted SST.

Restricting ourselves to subsets of the domain indicated in Figure 4 leads to instructive results. For example, when we consider restricted longitude ranges ((130E-160E, 30S-30N) and (160E-170W, 30S-30N)), we obtain essentially the same results as obtained for the full domain (not shown). Similarly, the results are essentially unchanged when we restrict ourselves to the latitude range 25S-25N. However, for latitude bands restricted to one hemisphere (0N-15N, and 0S-15S, for example), there is a dramatic increase in cirrus cloud area with cloud-weighted SST, and an even more dramatic increase in cumulus cloud top area with cloud-weighted SST. This is illustrated in Figure 7. The last result implies, as noted above, that we are no longer looking at a pure detrainment effect. Rather we are seeing the effect of convergence patterns changing, with convergence tending to maximize where temperature maximizes, although the existence of a temperature maximum in a restricted region does not necessarily coincide with a maximum in cloud-weighted SST in that region (Lindzen and Nigam, 1987). The different temperatures in Figure 7 are mostly due to temporal changes in SST. It is possible, that one might use both the variation of cumulonimbus coverage and cirrus coverage to back out the area effect even in the situation illustrated in Figure 7. For example, the percentage increase in cumulonimbus coverage is much greater than the increase in cirrus coverage – suggesting a reduction in detrainment with increasing temperature. However, for purposes of the present study, we decided that it was easier and less ambiguous to stick with regions where there was no significant overall trend in cumulonimbus activity.

We turn next to the radiative implications of such pronounced changes in the area of the cloudy/moist regions.

4. Simple radiative-convective assessment of feedback.

Before calculating the implications of the above for feedbacks, it is important to understand feedbacks more generally. Panel a of Figure 8 shows a schematic for the behavior of the climate system in the absence of feedbacks. The circle simply represents a node, while the box represents the climate system which is characterized by a no-feedback gain, G_0. The climate system acts on a radiative forcing, ΔQ, to produce a no-feedback response, $\Delta T_0=G_0\Delta Q$. Panel b shows the situation when a feedback process is present. Here, an additional forcing flux is produced which is proportional to the response, ΔT. This flux is written, $F\Delta T$, and is added to the external forcing, ΔQ. The response is now, $\Delta T=G_0(\Delta Q+F\Delta T)$. The quantity, $G_0F\Delta T$, is the (no-feedback) system response to the fed-back flux, $F\Delta T$. Solving for ΔT, one gets, $\Delta T=G_0Q/(1-G_0F)=\Delta T_0/(1-G_0F)$. The quantity, G_0F is sometimes referred to as the feedback factor, f; it is simply the response of the climate system to the fed-back flux (non-dimensionalized by 1C) resulting from ΔT=1C. Note, that the *net* response, ΔT, is not the same as the response to the fed-back flux alone. Note as well, that if there are several independent feedbacks, each will contribute its flux additively to the node, and f is replaced by Σf_i.

Thus, to evaluate the feedback factor due to changing the relative area of the cloudy/moist region, we must calculate the response of the climate system to such changes, all else being kept the same. This is readily dealt with using a very simple model. We divide the world into three regions: the cloudy/moist tropics, the clear/dry tropics, and the extratropics. This approach to the tropics is supported by the sharp transitions illustrated in Figure 1. The model is illustrated in Figure 9. We take each region to have a lapse rate of 6.5K/km. Both tropical regions are taken to have cloud capped trade cumulus boundary layers. Also, the tropical regions are both taken to have characteristic surface temperatures that are 10K warmer than the mean surface temperature, while the extratropical region is taken to have a characteristic surface temperature 10K colder than the mean surface temperature. We assume the current value of cloudy/moist fractional area to be 0.25, and choose the remaining parameters so as to be consistent with the global mean temperature, T_s, being 288K, and match ERBE observations (Barkstrom, 1984) which show a planetary reflectivity of 0.308, a tropical clear sky reflectivity of 0.13, a tropical reflectivity of 0.241, an extratropical reflectivity of 0.403, a planetary emission temperature of 254K, a tropical emission temperature of 259.1K, and an extratropical emission temperature of 249K. The cloudy/moist region is taken to have high relative humidity and high altitude cirrus, both of which lead to an elevated characteristic emission level. Consistent with the ERBE tropical emission level, we take the emission level for the cloudy/moist region to be at 10.6 km. and for the clear/dry region to be at 2.6 km. The characteristic emission level of the extratropics is taken to be at 4.5 km. The complete choice of parameters is given in Table 1. Although ERBE values don't completely constrain these choices, the precise choice of most individual parameters did not matter much to our final results as long as ERBE values were approximately matched. This was not entirely the case for the choice of tropical emission levels, and we will briefly discuss the sensitivity to different choices of the emission levels. Given the simplicity of the calculations, the interested reader can be readily check matters.

Table 1. Parameter selection in 3-box greenhouse model

Parameter	Description	Value
A_{cm}	Relative area of tropical moist/cloudy region	0.25
A_t	Relative area of the tropics	0.5
$A_d=A_t-A_{cm}$	Relative area of tropical dry region	0.25
$A_{et}=1-A_t$	Relative area of extratropics	0.5
f_h	Fractional coverage of high tropical clouds (within cloudy/moist region)	0.5
r_h	Reflectivity of high tropical clouds	0.35
f_l	Fractional coverage of tropical low cloud (trade cumuli, etc.)	0.265
r_l	Reflectivity of tropical low clouds	0.41
r_{bt}	Clear sky reflectivity in the tropics	0.13
r_{tet}	Total reflectivity for the extratropics	0.403
T_s	Mean surface temperature	
$T_{st}=T_s+10K$	Tropical surface temperature	
$T_{set}=T_s-10K$	Extratropical surface temperature	
$T_{ecm}=T_{st}-68.8K$	Emission temperature from tropical moist region	
$T_{ed}=T_{st}-17K$	Emission temperature from tropical dry region	
$T_{eet}=T_{set}-29.3K$	Emission temperature from extratropics	
Q_0	Mean solar irradiation	$\sigma(254K)^4/(1-0.308)$
Q_t	Relative solar irradiation in tropics	1.174
Q_{et}	Relative solar irradiation in extratropics	0.826
$f_{tcm}=f_h+(1-f_h)f_l$	Total fractional cloud coverage in tropical moist region	

The information in Table 1 permits us to calculate total reflectivity in each of the three regions, from which we can then calculate the net incoming solar radiation:

Total reflectivity in tropical cloud/moist region = $r_{tcm} = f_h r_h+(1-f_h) f_l r_l+(1-f_{tcm}) r_{bt}$

Total reflectivity in tropical dry region = $r_{td} = f_l r_l + (1-f_l) r_{bt}$

The total reflectivity for the extratropics is simply taken from ERBE, and the value is given in Table 1.

Net incoming solar radiation = $Q = Q_0 (Q_t (A_{cm}(1-r_{tcm}) + A_d(1-r_{td})) + A_{et} Q_{et}(1-r_{tet}))$, and net reflectivity will simply be $(1-Q/Q_0)$.

The net OLR consists simply in Planck Black Body emission from the characteristic emission levels in the three regions:

Net OLR = $C(T_s) = \sigma(A_{cm} T_{ecm}^4 + A_d T_{ed}^4 + A_{et} T_{eet}^4)$

Note that convective adjustment, here, consists in fixing the relation between surface temperature and the temperature at the characteristic emission levels.

Finally, we obtain the mean surface temperature by equating net incoming solar radiation to net OLR:

$C(T_s) = Q$ Y T_s

Once one obtains values for the various variables that lead to the present climate (i.e., T_s=288K, Total reflectivity = $(1- Q/Q_0)$ =0.308, etc.), one then varies the relative areas of the cloudy/moist and clear/dry regions, keeping the total area of the tropics fixed. Figure 10 shows how the global mean temperature varies with the fractional area of the cloudy/moist region. It also shows how the global reflectivity varies. The latter varies fairly little since substantial reflectivity is due to the clouds capping the boundary layer and to the surface reflectivity. However, the global mean radiative-convective surface temperature varies substantially indicating the strong dominance of the infrared effect of the cloudy/moist region. Roughly speaking, a 15% reduction in this area (from a base of about 0.25) leads to about a 1.7K reduction in global mean temperature. Note that the cloudy/moist region is not totally cloud covered; rather, we assume that f_h is fixed so that upper level cloudiness ($f_h * A_{cm}$) and the area of cloudy/moist air (A_{cm}) are proportional to each other.

Now, our results shown in Figure 5 imply that a 15% reduction in the cloudy/moist area results from a 1K increase in cloud-weighted surface temperature. Under conditions of global warming, we assume that both global mean temperature and cloud-weighted surface temperature increase together. Given that an increase in surface temperature leads to a reduction of cloudy/moist area, while such a reduction leads to a decrease in radiative-convective equilibrium mean temperature, we have a negative feedback. As shown in the figure, the response to a 15% reduction in cloudy/moist area is a reduction of T_s from 288K to 286.3K, or a feedback factor (G_0F or f) of -1.7. *Essentially, the cloudy/moist region appears to act as an infrared adaptive iris which opens up and closes down the clear/dry regions, which effectively permit infrared cooling, in such a manner as to resist changes in tropical surface temperature.* Our model includes the fact that dynamics ties temperatures everywhere together and determines the mean meridional

gradient. The feedback factor is for the effect of the tropics on the global mean. Feedbacks in the extratropics are taken as neutral. Thus, the response to a doubling of CO_2, which in the absence of feedbacks is expected to be about 1.2K, would be reduced to 0.44K due to the iris effect. In some respects, the iris effect can be considered to be independent of the positive feedbacks found in current models. Climate models sensitive to external radiative forcing tend to have a feedback factor of about 0.2 for extratropical clear-sky water vapor, 0.1 for extratropical clouds, and 0.1 for snow/ice, resulting in a total extratropical feedback factor of 0.4 (Lindzen, 1993, Schneider et al, 1999). Less sensitive models have f_{model} (extratropical)−0.1. In the presence of the iris feedback, even the presence of the feedbacks from the more sensitive models would only reduce the total negative feedback factor from -1.7 to -1.3 and increase the response from 0.44K to 0.52K. The feedbacks from the less sensitive models would do even less. This is illustrated in Table 2. (Note that although we retain 3 significant figures for convenience in computation, nothing in the data suggests this level of accuracy.) Table 2 considers the possibility that the iris feedback might be more or less than estimated. For example, the iris feedback factor can be reduced to -1 by increasing the emission temperature from the tropical cloudy/moist region to T_{st} - 57.26K while decreasing the emission temperature for the tropical clear/dry region to T_{st} - 24K (corresponding to approximate emission levels of 8.8km and 3.7km). On the other hand, the assumption fixed effective emission levels and constant lapse rate in the tropical cloudy/moist region is an inexact simplification that probably leads us to underestimate the negative feedback since when SST (or cloud-weighted SST) increases, high cloud/humidity decreases, and the emission level should descend. Moreover, for a moist adiabatic lapse rate, the upper tropospheric temperature should increase more than that of SST.

Table 2. Modification of climate sensitivity in presence of both model feedbacks and various modifications of the iris feedback.

Iris Feed-back Factor (f)	GCM Feed-back Factor (f) (high)	GCM Feed-back Factor (f) (low)	Total Feed-back Factor (f) (high)	Total Feed-back Factor (f) (low)	Net Gain (1/(1-f)) (high)	Net Gain (1/(1-f)) (low)	Re-sponse to $2xCO_2$ (°C) (high)	Re-sponse to $2xCO_2$ (°C) (low)
-3	0.4	0.1	-2.6	-2.9	0.278	0.256	0.336	0.308
-2	0.4	0.1	-1.6	-1.9	0.385	0.345	0.462	0.414
-1	0.4	0.1	-0.6	-0.9	0.625	0.526	0.75	0.631
-0.5	0.4	0.1	-0.1	-0.4	0.909	0.714	1.091	0.857

Such low estimates for sensitivity are consistent with the independent estimates based on the response to sequences of volcanos (Lindzen and Giannitsis, 1998). Even assuming GCM clear-sky water vapor feedbacks are correct for the tropics would only add another 0.2 to the total feedback factors – resulting in slight increases in the above responses.

5. GCM assessment.

An attempt to replicate the presence of the feedback using a GCM consisting in the NCAR (National Center for Atmospheric Research) CCM3 (Community Climate Model, Version 3) physics and a dynamic core developed by S.J. Lin at NASA/Goddard, forced by the same SST data used for the observational analysis, fails to indicate its presence. A comparison of observational and model results for the period May-June 1998 is given in Figure 11. The GCM scatter suggests no systematic response of cloud area to cloud weighted SST although the formal regression actually suggests a positive rather than a negative dependence. Comparisons with other models (the COLA (Center for Ocean, Land, Atmospheres) and several versions of NCAR's CCM3 models have been examined so far) also shows profound differences from observations regardless of whether diagnostic or prognostic cloud formulations were used. However, the modes of failure differ somewhat from model to model. Detailed comparisons will be made in a separate paper in which we hope to have additional model comparisons.

The failure of models to replicate observed relations between upper cloud coverage and cloud weighted SST suggests that models may be failing to produce a major negative feedback. We still have not examined the relation between upper cloud coverage and relative humidity in order to see if the origin of tropical free tropospheric humidity is properly handled within models. However, at least some models fail to show the sharp delineation between cloudy/moist and clear/dry regions, and most models overestimate humidity in the clear/dry regions (Bates and Jackson, 1997).

6. Discussion.

Given the limited period and region considered as well as the incompleteness of spectral data at suitable spectral, temporal and spatial resolution, and the limitations of the SST data, the present results must still be regarded as tentative. There remain, as well, the possibilities that under conditions of global warming due to increasing CO_2, that CAPE might change as might the amount of convection (although the present results suggest that the second possibility is small unless accompanied by changes in the pattern of SST). If CAPE increases, the time available for rain formation would decrease, and this might diminish the present feedback. There are indeed arguments and observations that suggest modest increases for warmer climates (Emanuel and Bister, 1996, Rennó, 1997). Nonetheless, given the low climate sensitivity implied by the iris effect, and the plausible expectation that differences in CAPE comparable to what might be expected from future climate change are to be found within the region shown in Figure 4, we would not expect the iris effect to be significantly reduced under conditions of doubled CO_2.

We are thus left with significant evidence for a very effective negative feedback in the tropics. This by no means argues against the possibility of large climate change. However, it implies that such changes will, as earlier proposed in Lindzen (1993), demand a change in those factors which determine the equator to pole temperature difference such as changes in the intensity of the Hadley supply of momentum to the subtropical jet (Lindzen and Pan,1993, Hou, 1998) or changes in the differential heating as might be produced by large scale high latitude snow cover or changes in the ocean heat transport. In the absence of such changes, strong negative feedbacks

in the tropics will also constrain global temperatures. On the other hand, the existence of a strong negative feedback in the tropics will act in such a manner as to translate changes in the dynamic heat flux between the tropics and the extratropics into changes in the global mean temperature rather than simple self-cancelling changes in the tropics and extratropics. Thus, it is by no means clear that the thermostatic process described in this paper will not increase natural variability in global mean temperature – in contrast to the findings of Hall and Manabe (1998).

Whether the iris feedback ultimately proves as effective as our results suggest, the inability of existing models to replicate the relevant observations suggests the need for model improvement in an area potentially crucial to the determination of climate sensitivity. It also suggests that the range of climate sensitivity found in current models need not constrain the real range – especially at the low end. The present results suggest the importance of improved data (including, for example 183 GHz sounders on geostationary satellites so as to obtain observations of water vapor at the same time and space resolution as the cloud data) in order to more firmly identify the nature and magnitude of the feedback whose discovery is described in the present paper. Finally, it would be interesting to develop a parameterization of the process discussed in this paper for implementation in a GCM so as to see how the climate behavior of the model would be altered. This would address the challenge put forth in Held and Soden (2000); namely that explicit processes be suggested that might reduce the water vapor feedback so that these processes could be checked in GCMs. It would, of course, be of interest to see how model climate sensitivity is affected. However, it is likely to be of comparable interest to see how the parameterization affects such matters as air-sea coupling and climate drift.

Acknowledgments.

The efforts of R.S. Lindzen were supported by grants ATM9813795 from the National Science Foundation, DEFG02-93ER61673 from the Department of Energy, and NAG5-5147 from National Aeronautics and Space Administration. The work of M.-D. Chou was supported by the Radiation Research Program, NASA/Office of Earth Science. We would like to thank Dr. S.J. Lin and Ms. Sharon Nebuda for providing the NASA/NCAR results used in Figure 11, Drs. E. Schneider and B. Boville for assessing of the COLA and NCAR models respectively for our mechanism, and Dr. D. Kirk-Davidoff for helpful comments.

References.

Barkstrom, B.R. (1984) The Earth Radiation Budget Experiment (ERBE), *Bull. Amer. Met. Soc.*, **65**, 1170-1185.

Bates, J.J. and D.L. Jackson (1997) A comparison of water vapor measurements with AMIP 1 simulations. J. Geophys. Res., 102, 21837-21852.

Betts, A.K. (1990) Greenhouse warming and the tropical water budget. *Bull. Amer. Met. Soc.*, **71**, 1464-1465.

Emanuel, K.A., and M. Bister, 1996: Moist convective velocity and buoyancy scales. *J. Atmos. Sci.*, **53**, 3276--3285.

Emanuel, K.A. and R.T. Pierrehumbert (1996) Microphysical and dynamical control of tropospheric water vapor. NATO ASI Ser., 135, Clouds, Chemistry and Climate (Editors: P.J. Crutzen and V. Ramanathan), Springer Verlag, Berlin.

Fairall, C. W., E. F. Bradley, D. P. Rogers, J. B. Edson, and G. S. Young, 1996: Bulk parameterization of air-sea fluxes for TOGA COARE. J. Geophy. Res., 101, 3747-3764.

Gamache J.F. and R.A. Houze, 1983: Water budget of a meso-scale convective system in the tropics. *J. Atmos. Sci.*, **40**, 1835-1850.

Hall, A. and S. Manabe, 1999: The role of water vapor feedback in unperturbed climate variability and global warming. *Journal of Climate*, **12**, 2327-2346.

Held, I.M., and B. Soden (2000) Water vapor feedback and global warming, *Annual Reviews of Energy and the Environment*, in press

Hou, A.Y., 1998: Hadley circulation as a modulator of the extratropical climate. *J. Atmos. Sci.*, **55**, 2437-2457.

Lindzen, R.S. (1990) Response: Greenhouse warming and the tropical water budget. *Bull. Amer. Met. Soc.*, **71**, 1465-1467.

Lindzen, R.S. (1993) Climate dynamics and global change. *Ann. Rev. Fl. Mech.*, **26**, 353-378.

Lindzen, R.S. and S. Nigam (1987) On the role of sea surface temperature gradients in forcing low level winds and convergence in the tropics. *J. Atmos. Sci.*, **44**, 2418-2436.

Lindzen, R.S., and W. Pan (1994) A note on orbital control of equator-pole heat fluxes. *Clim. Dyn.*, **10**, 49-57.

Lindzen, R.S. and C. Giannitsis (1998) The response to volcanos singly and in sequence as a test of climate models. *J. Geophys. Res.*, **103**, 5929-5941.

Manabe, S. and Wetherald, R. T. 1967: Thermal equilibrium of the atmosphere with a given distribution of relative humidity. *J. Atmos. Sci.*, **24**, 241 - 259.

Miller, R. and R.S. Lindzen (1992) Organization of rainfall by an unstable jet with application to African waves. *J. Atmos. Sci.*, **49**, 1523-1540.

Pierrehumbert, R.T., 1995: Thermostats, Radiator Fins and the Local Runaway Greenhouse, *J. Atmos. Sci.*, **52**, 1784-1806.

Prabhakara, C., D. P. Kratz, J.-M. Yoo, G. Dalu, and A Vernekar, 1993: Optically thin cirrus clouds: Radiative impact on the warm pool. *J. Quan. Spectrosc. Radiat. Transfer,* **49**, 467-483.

Rennó, N.O., 1997. Multiple Equilibria in Radiative-Convective Atmospheres. *Tellus*, **49A**, 423-438.

Reynolds, R. W. and T. M. Smith, 1994: Improved global sea surface temperature analyses. J. Climate, 7, 929-948.

Riehl, H. and J. S. Malkus, 1958: On the heat balance in the equatorial trough zone. *Geophysica* (Helsinki), **6**, 503-538.

Rogers, R.R. and M.K. Yau, 1989: *A Short Course in Cloud Physics*. Pergamon Press, London, 293 pp.

Salathé, E.P. and D.L. Hartmann (1997) A trajectory analysis of tropical upper-tropospheric moisture and convection. *J. Climate*, **10**, 2533-2547.

Sherwood, S.C. (1996) Maintenance of free-tropospheric water vapor distribution. Part II: simulation by large-scale advection. *J. Climate*, **9**, 2919-2934.

Schneider, E.K., B.P. Kirtman and R.S. Lindzen (1999) Upper tropospheric water vapor and climate sensitivity. *J. Atmos. Sci.*,**56**, 1649-1658.

Soden, B.J. 1998: Tracking upper tropospheric water vapor. *J. Geophys. Research* 103,17069-17081.

Spencer, R.W., Braswell, W.D. 1997: How dry is the tropical free troposphere? Implications for global warming theory. *Bull. Am Meteorol Soc*, **78**, 1097-1106.

Stephens, G.L., Jackson, D.L.,Wittmeyer, I. (1996) Global observations of upper tropospheric water vapor derived from TOVS radiance data. *J. Climate*, **9**, 305-326.

Straus, D. and R.S. Lindzen (2000) Planetary scale baroclinic instability and the MJO. accepted *J. Atmos. Sci.*

Sun, D-Z. and R.S. Lindzen (1993) Distribution of tropical tropospheric water vapor. *J. Atmos. Sci.*, **50**, 1643-1660.

Udelhofen, P.M. and Hartmann, D.L. (1995) Influence of tropical cloud systems on the relative humidity in the upper troposphere. *J. Geophys. Res.*, **100**, 7423-7440.

Figure Legends.

Figure 1. Retrieval of relative humidity for the 500mb-300mb layer on May 5, 1995 from SSM/T-2 183GHz soundings. Courtesy of Roy Spencer. See Spencer and Braswell (1997) for details of the measurement.

Figure 2. Schematic illustrating the moisturization of underlying air by precipitation from cirrus outflow of cumulonimbus clouds.

Figure 3. Schematic illustrating change in cloud-weighted SST due to cloud systems moving from the central position to colder and warmer regions. Dotted horizontal lines correspond to isotherms. Units are nominally deg C.

Figure 4. Region used for present study.

Figure 5. Scatter plots showing how cirrus coverage varies with cloud-weighted SST (see text for details).

Figure 6. Scatter plots showing how cumulonimbus coverage varies with cloud-weighted SST (see text for details).

Figure 7. Scatter plots showing how cirrus and cumulus coverage varies with cloud-weighted SST for a subregion of Figure 4 (15S-Equator, 130E-170W; see text for details).

Figure 8. Schematic illustrating operation of feedbacks.

Figure 9. Three-region model for 2-dimensional calculation of radiative-convective equilibrium. Symbols are defined in Table 1.

Figure 10. Calculated variation of global mean temperature, Ts, v. area (relative to the entire globe) of the tropical cloudy/moist region.

Figure 11. Scatter plots showing how cirrus coverage varies with cloud-weighted SST for both observations and the DAO climate GCM forced by the observed SST (see text for details).

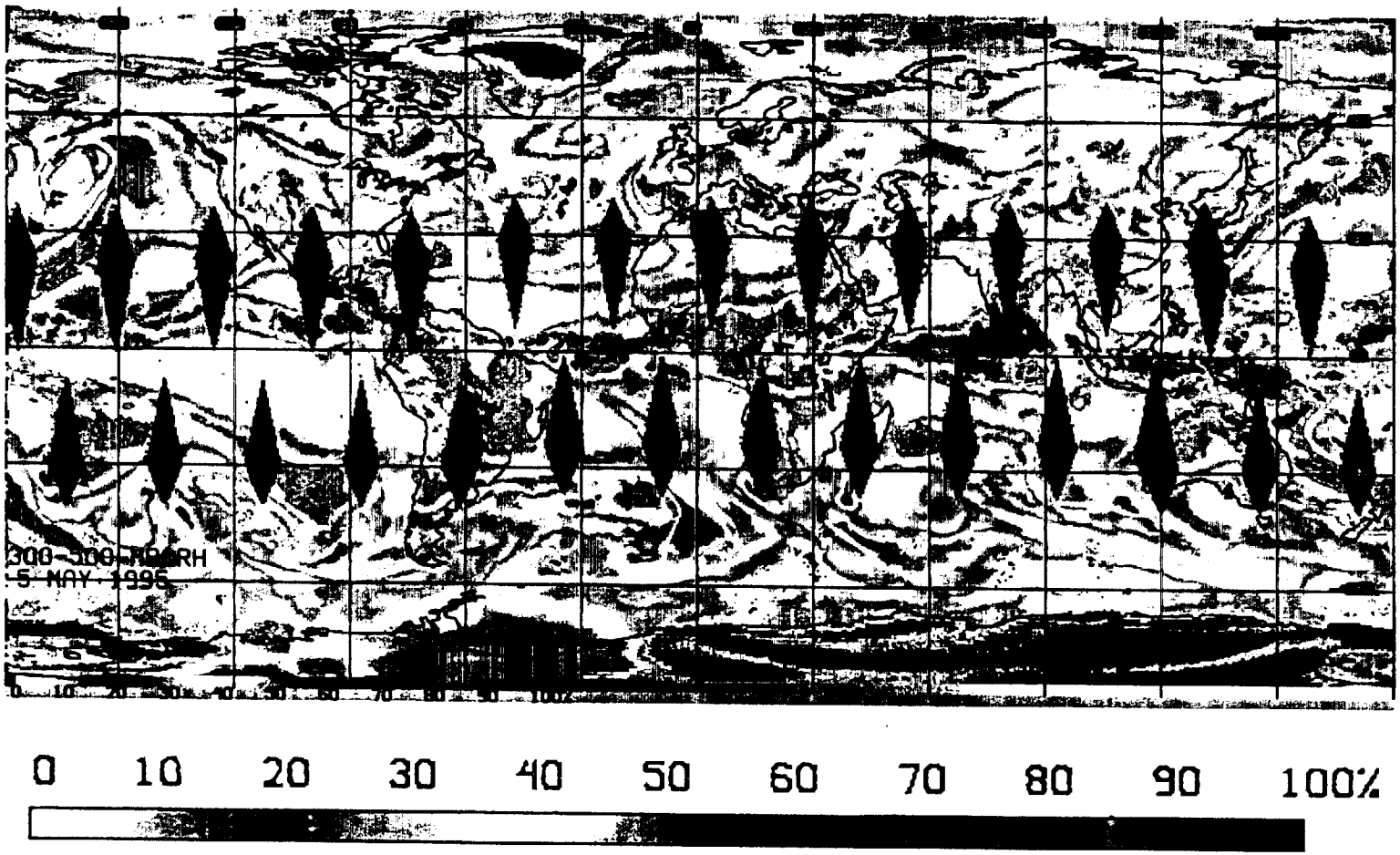

Figure 1

May 5, 1995

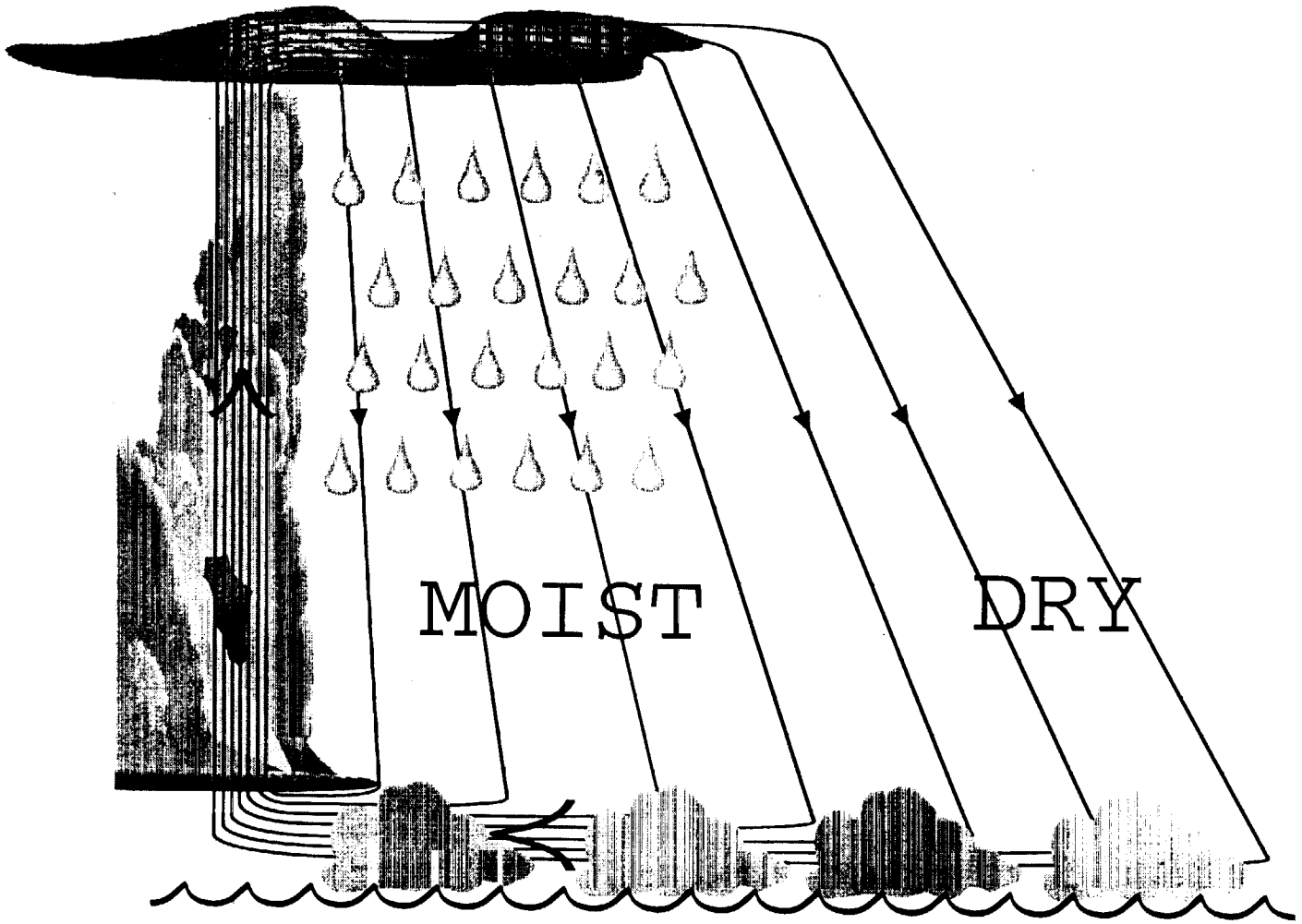
MOIST
DRY

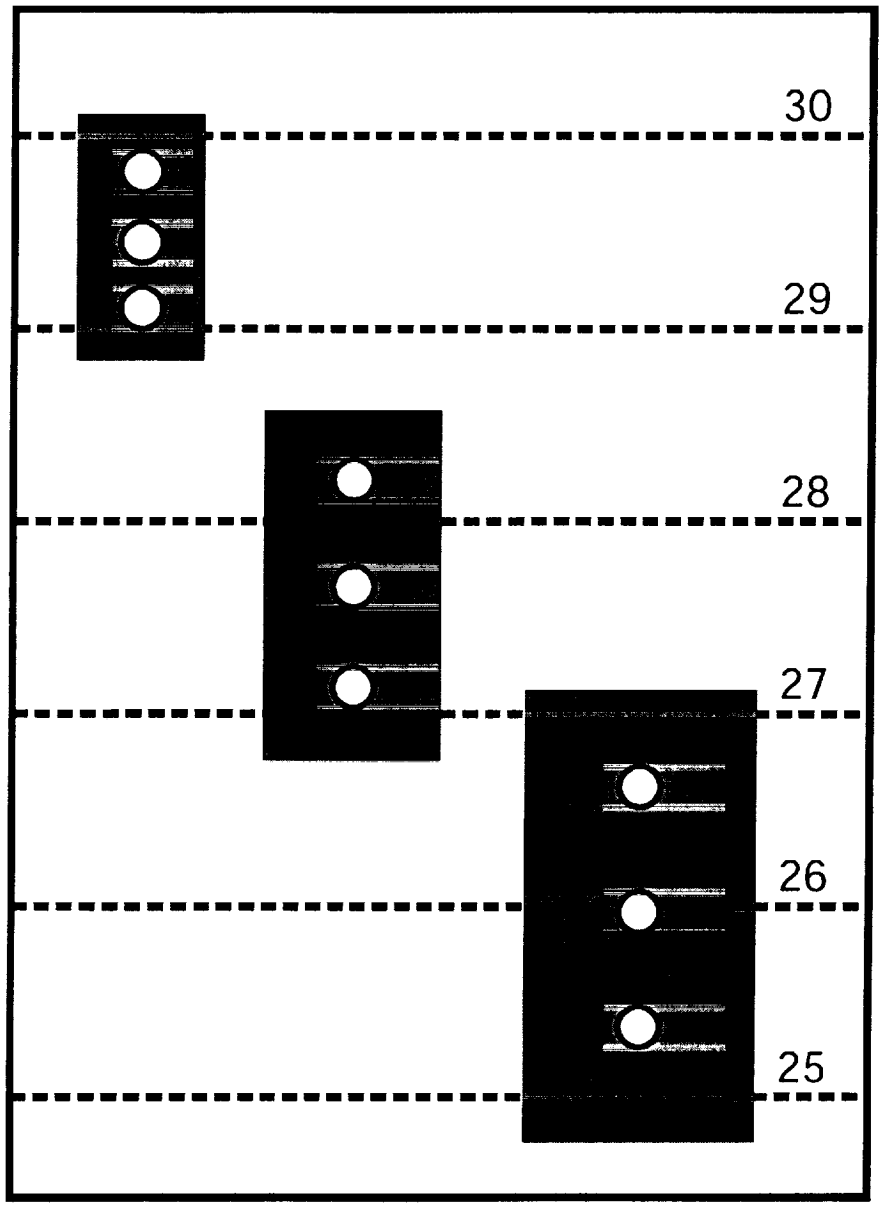

Upper Level Cirrus

Cumulonimbus

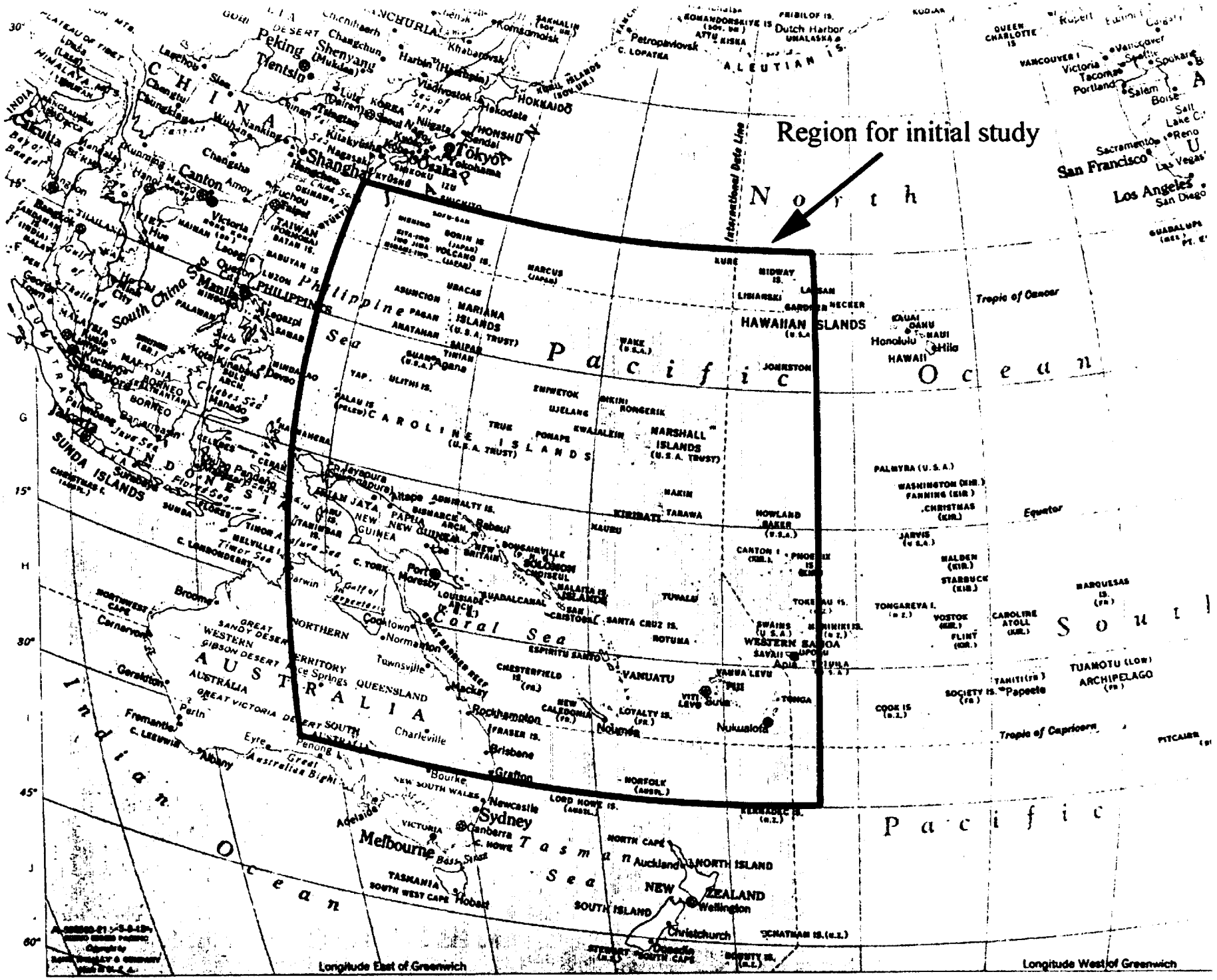
Region for initial study
North Pacific Ocean
South Pacific Ocean
Indian Ocean
Coral Sea
Tasman Sea
Philippine Sea
South China Sea
AUSTRALIA
CHINA
INDONESIA
NEW ZEALAND
HAWAIIAN ISLANDS
MARIANA ISLANDS
CAROLINE ISLANDS
MARSHALL ISLANDS
Tropic of Cancer
Tropic of Capricorn
Equator
International Date Line
Longitude East of Greenwich
Longitude West of Greenwich

Figure 3 4

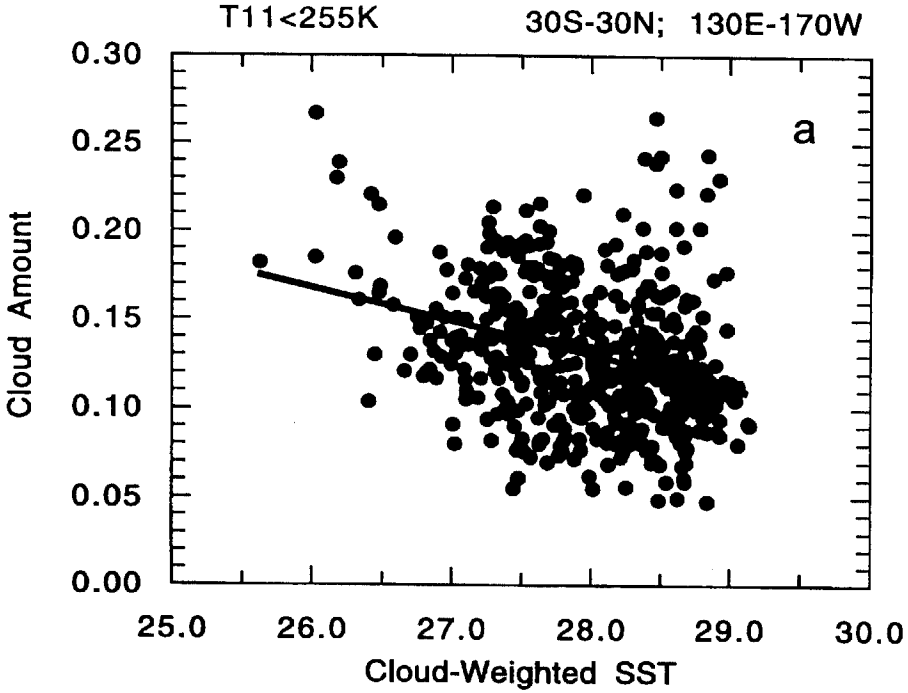
T11<255K
30S-30N; 130E-170W
a
Cloud Amount
0.30
0.25
0.20
0.15
0.10
0.05
0.00
25.0
26.0
27.0
28.0
29.0
30.0
Cloud-Weighted SST

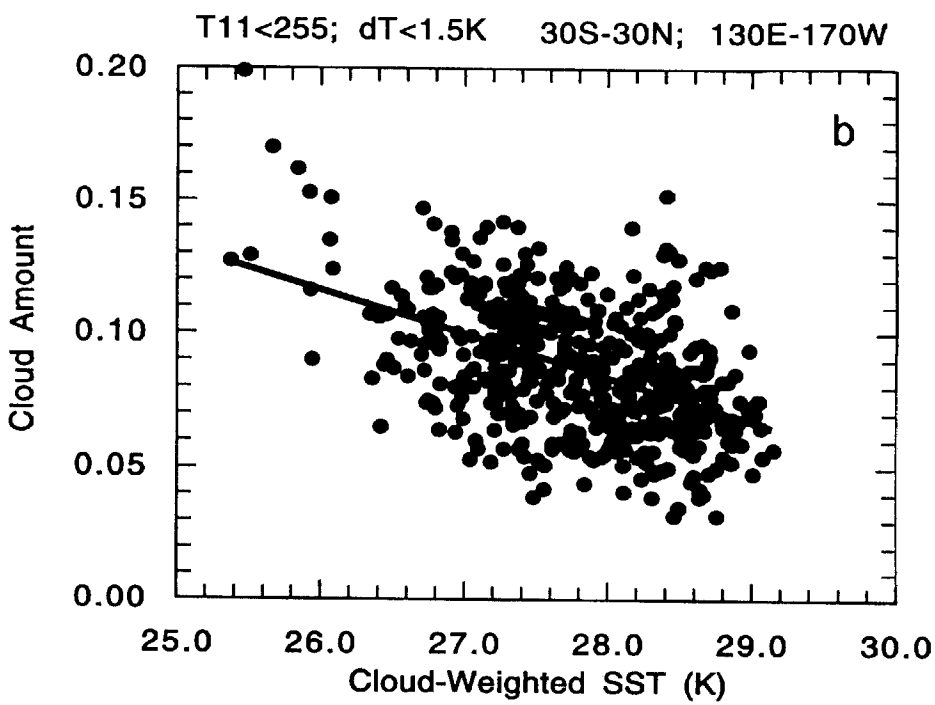
T11<255; dT<1.5K
30S-30N; 130E-170W
b
Cloud Amount
0.20
0.15
0.10
0.05
0.00
25.0
26.0
27.0
28.0
29.0
30.0
Cloud-Weighted SST (K)

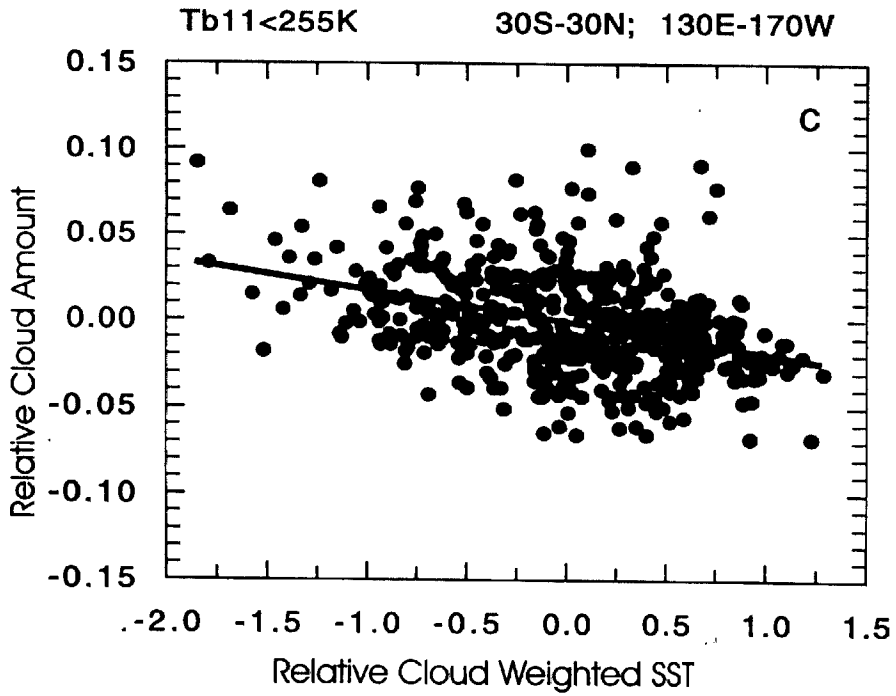
Tb11<255K
30S-30N; 130E-170W
c
Relative Cloud Amount
0.15
0.10
0.05
0.00
-0.05
-0.10
-0.15
-2.0
-1.5
-1.0
-0.5
0.0
0.5
1.0
1.5
Relative Cloud Weighted SST

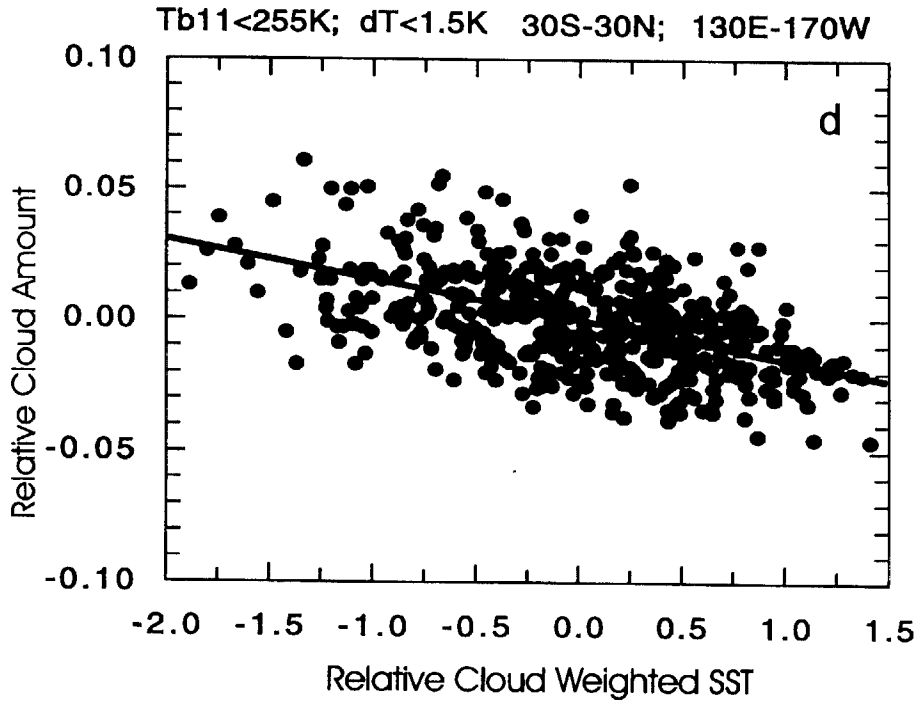
Tb11<255K; dT<1.5K
30S-30N; 130E-170W
d
Relative Cloud Amount
0.10
0.05
0.00
-0.05
-0.10
-2.0
-1.5
-1.0
-0.5
0.0
0.5
1.0
1.5
Relative Cloud Weighted SST

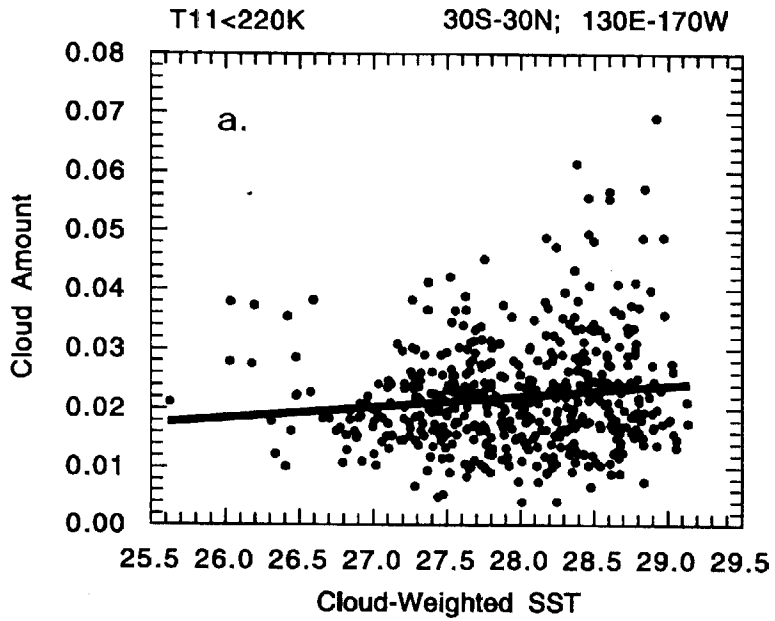
T11<220K
30S-30N; 130E-170W
a.
Cloud Amount
0.08
0.07
0.06
0.05
0.04
0.03
0.02
0.01
0.00
25.5 26.0 26.5 27.0 27.5 28.0 28.5 29.0 29.5
Cloud-Weighted SST

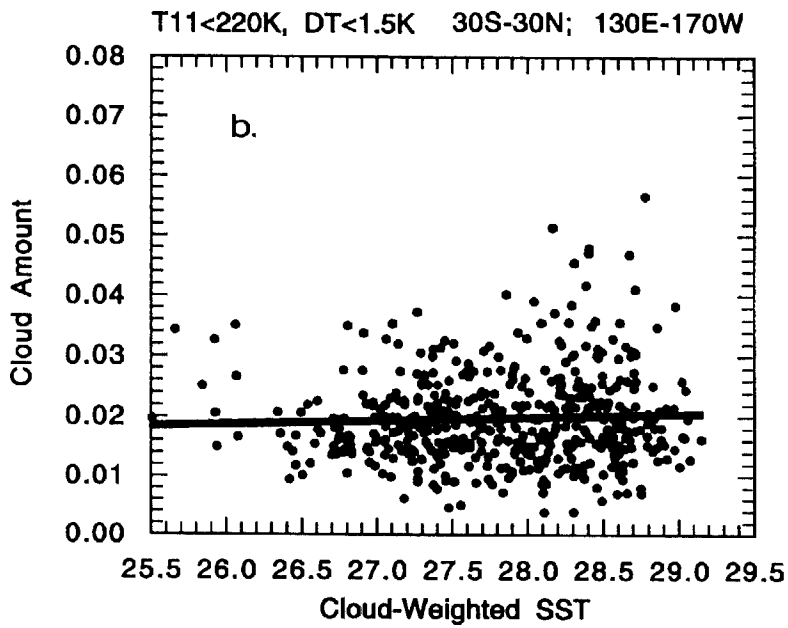
T11<220K, DT<1.5K
30S-30N; 130E-170W
b.
Cloud Amount
0.08
0.07
0.06
0.05
0.04
0.03
0.02
0.01
0.00
25.5 26.0 26.5 27.0 27.5 28.0 28.5 29.0 29.5
Cloud-Weighted SST

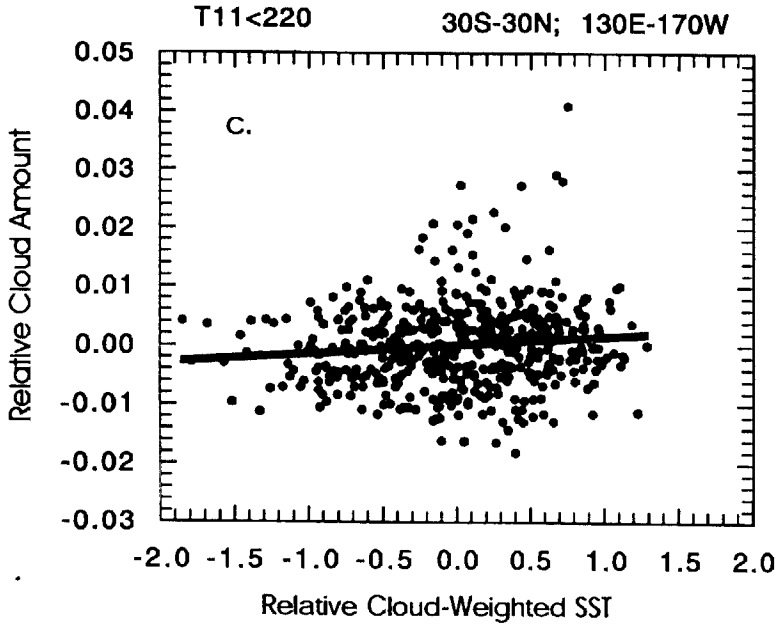
T11<220
30S-30N; 130E-170W
c.
Relative Cloud Amount
0.05
0.04
0.03
0.02
0.01
0.00
-0.01
-0.02
-0.03
-2.0 -1.5 -1.0 -0.5 0.0 0.5 1.0 1.5 2.0
Relative Cloud-Weighted SST

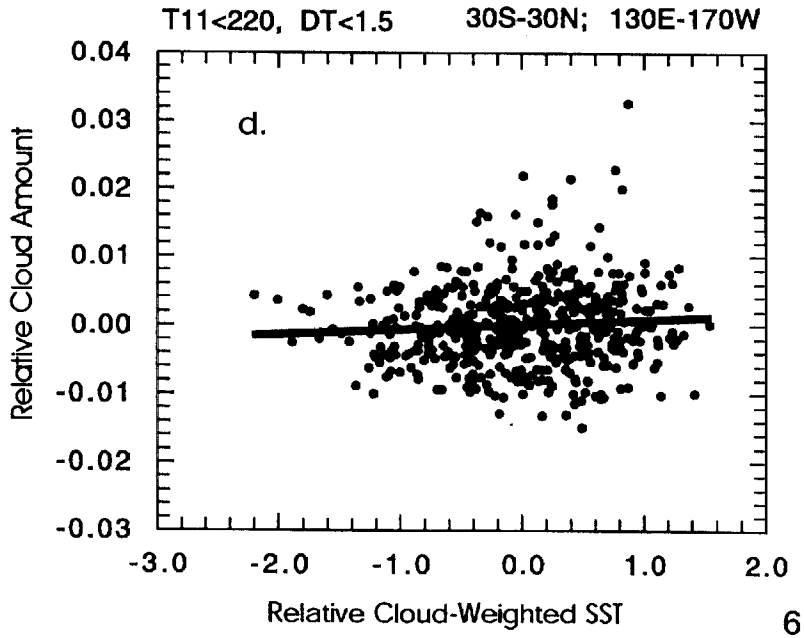
T11<220, DT<1.5
30S-30N; 130E-170W
d.
Relative Cloud Amount
0.04
0.03
0.02
0.01
0.00
-0.01
-0.02
-0.03
-3.0 -2.0 -1.0 0.0 1.0 2.0
Relative Cloud-Weighted SST

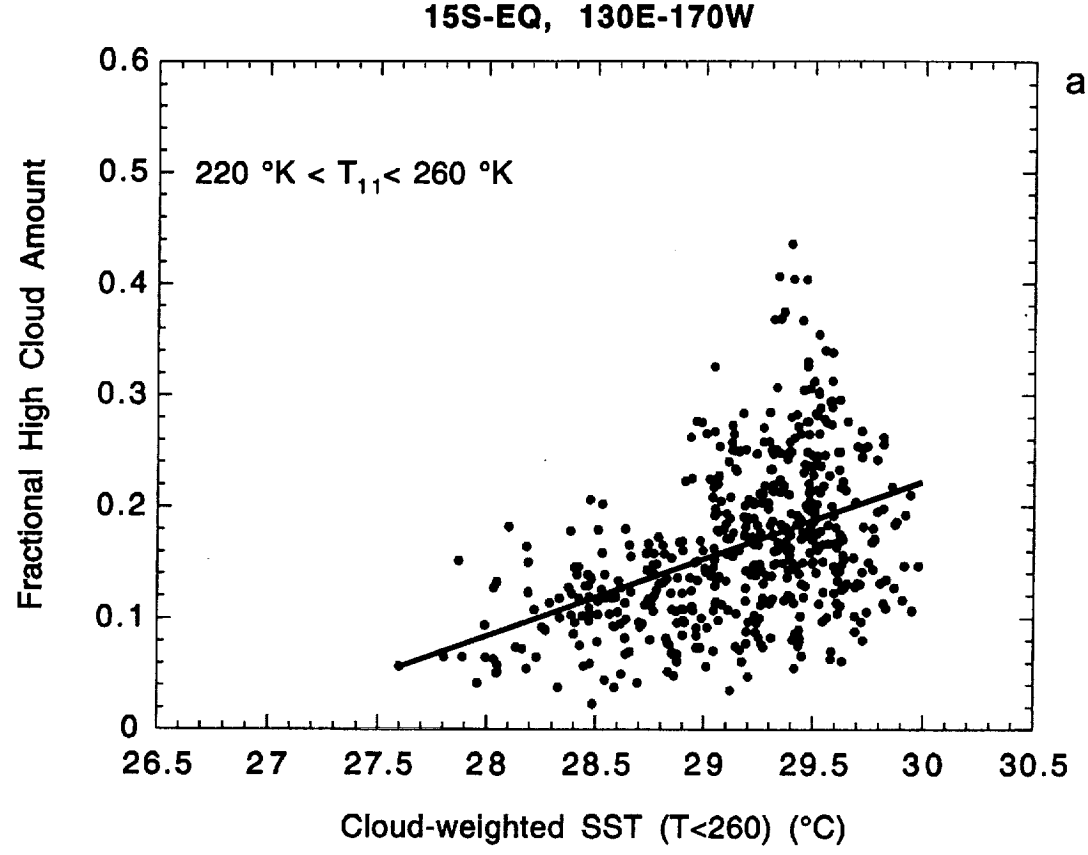
15S-EQ, 130E-170W
a
220 °K < T11< 260 °K
Fractional High Cloud Amount
0.6
0.5
0.4
0.3
0.2
0.1
0
26.5
27
27.5
28
28.5
29
29.5
30
30.5
Cloud-weighted SST (T<260) (°C)

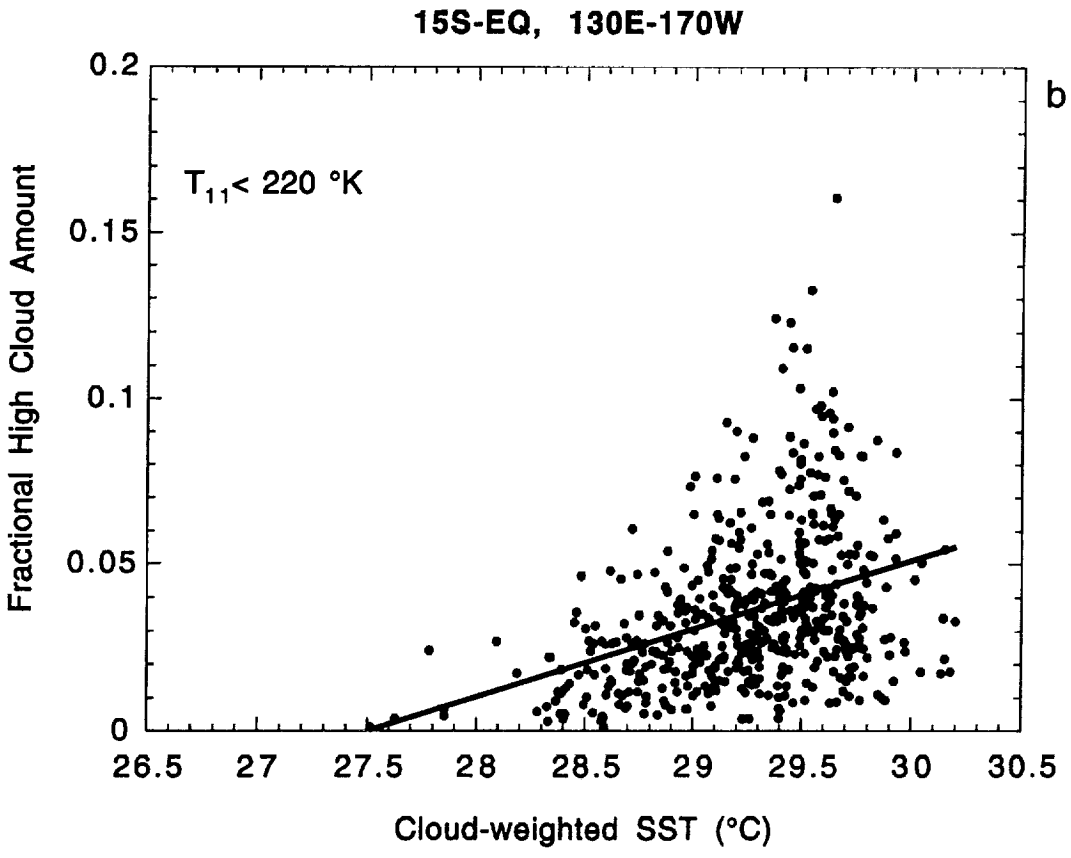
15S-EQ, 130E-170W
b
T11< 220 °K
Fractional High Cloud Amount
0.2
0.15
0.1
0.05
0
26.5
27
27.5
28
28.5
29
29.5
30
30.5
Cloud-weighted SST (°C)

a. No Feedback Case

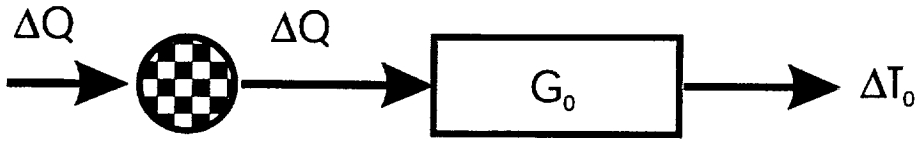

$$\Delta T_0 = G_0 \Delta Q$$

b. Feedback Case

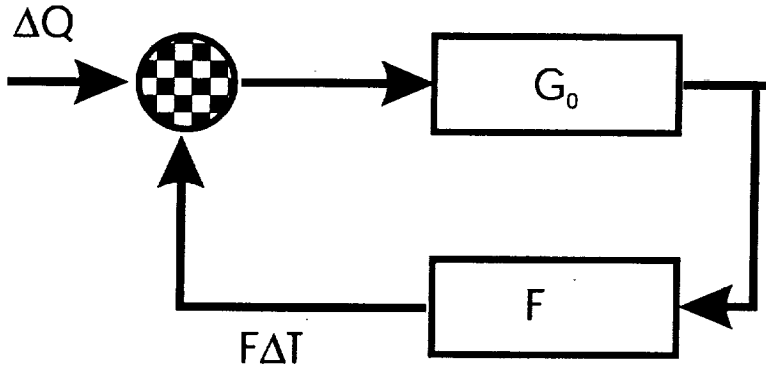

$$\Delta T = G_0(\Delta Q + F\Delta T)$$

$$\Delta T = \frac{G_0 \Delta Q}{(1 - G_0 F)}$$

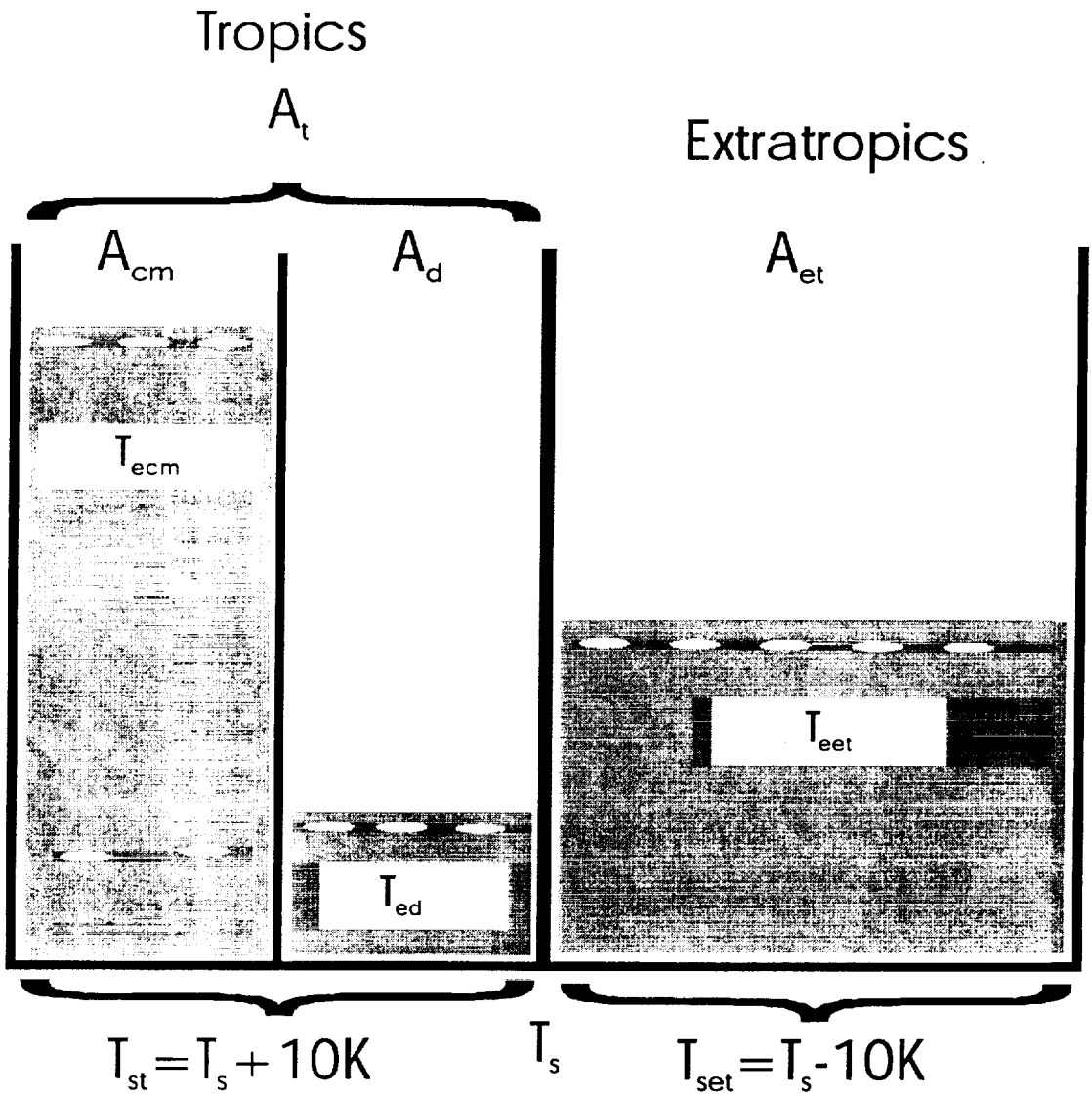

Simple three-box model for the Greenhouse Effect due to clouds and water vapor

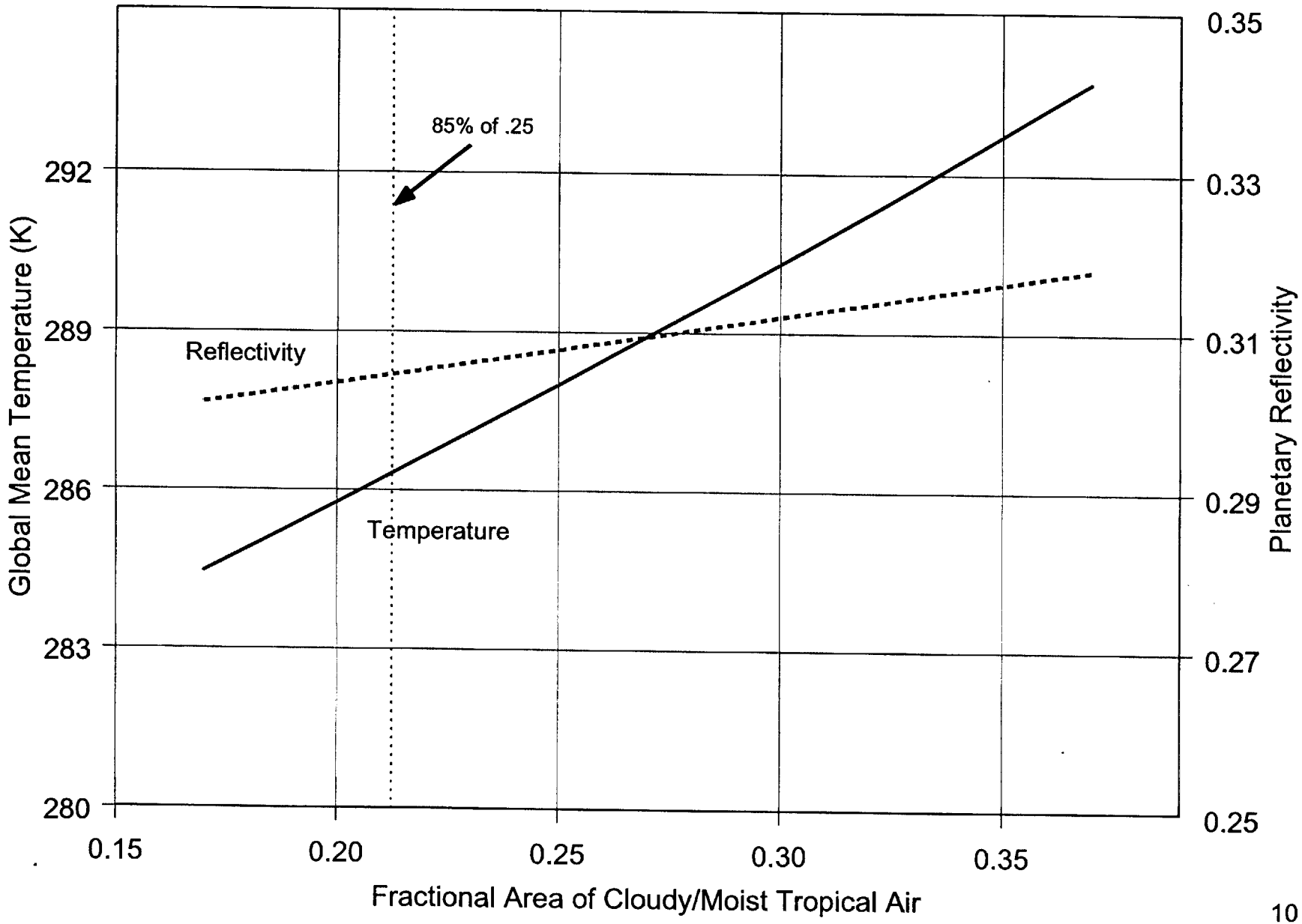
85% of .25
Reflectivity
Temperature
Global Mean Temperature (K)
292
289
286
283
280
0.15
0.20
0.25
0.30
0.35
Fractional Area of Cloudy/Moist Tropical Air
0.35
0.33
0.31
0.29
0.27
0.25
Planetary Reflectivity

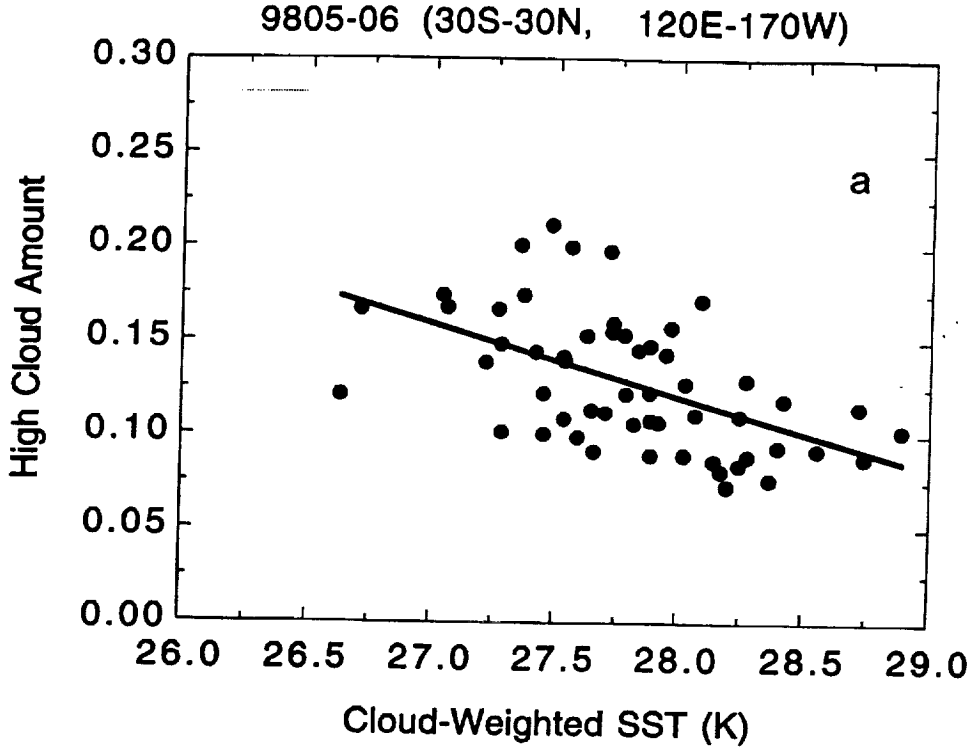
9805-06 (30S-30N, 120E-170W)
0.30
0.25
0.20
0.15
0.10
0.05
0.00
High Cloud Amount
a
26.0
26.5
27.0
27.5
28.0
28.5
29.0
Cloud-Weighted SST (K)

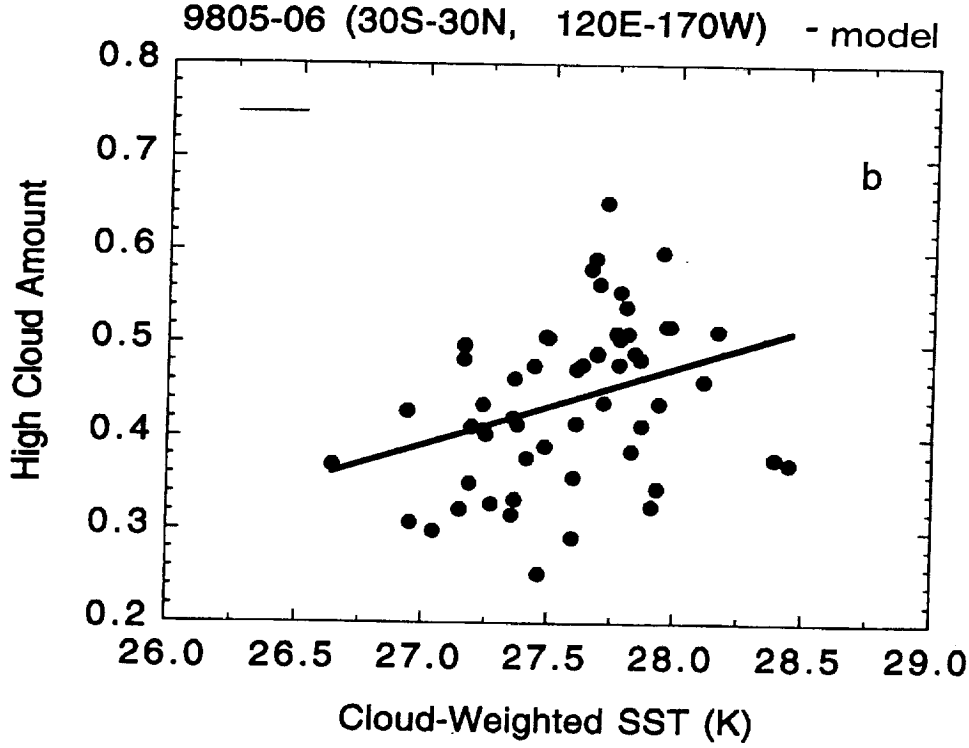
9805-06 (30S-30N, 120E-170W) - model
0.8
0.7
0.6
0.5
0.4
0.3
0.2
High Cloud Amount
b
26.0
26.5
27.0
27.5
28.0
28.5
29.0
Cloud-Weighted SST (K)